RSC Advances

This is an *Accepted Manuscript*, which has been through the Royal Society of Chemistry peer review process and has been accepted for publication.

Accepted Manuscripts are published online shortly after acceptance, before technical editing, formatting and proof reading. Using this free service, authors can make their results available to the community, in citable form, before we publish the edited article. This *Accepted Manuscript* will be replaced by the edited, formatted and paginated article as soon as this is available.

You can find more information about *Accepted Manuscripts* in the Information for Authors.

Please note that technical editing may introduce minor changes to the text and/or graphics, which may alter content. The journal's standard Terms & Conditions and the Ethical guidelines still apply. In no event shall the Royal Society of Chemistry be held responsible for any errors or omissions in this *Accepted Manuscript* or any consequences arising from the use of any information it contains.

ROYAL SOCIETY OF CHEMISTRY

www.rsc.org/advances

Carbon-coated SnO_2 thin films developed by magnetron sputtering as anode material for lithium-ion batteries

Yu Zhang [a], Hong Zhang [a], Jia Zhang [a], Jiaxi Wang [a], Zhicheng Li [a, b, *]

[a] School of Materials Science and Engineering, Central South University, Changsha 410083, P.R. China

[b] State Key Laboratory of Powder Metallurgy, Central South University, Changsha 410083, P.R.China

ABSTRACT

Magnetron sputtering technique was employed to produce carbon-coated SnO_2 (CCSO) thin films, which were applied as anode material for lithium-ion batteries (LIBs). The CCSO performs better electrochemical properties than the pure SnO_2 material. The CCSO thin film has a specific discharge capacity of 650 $mAh \cdot g^{-1}$ with a capacity retention rate of 72% after 100 cycles, while the pure SnO_2 has only 207 $mAh \cdot g^{-1}$ with a capacity retention rate of 19%. High-resolution transmission electron microscopic analysis provides crucial information that magnetron-sputtered carbon coating has an amorphous feature and shows excellent durability that the carbon film coated tightly on the surface of the SnO_2 active materials through the discharging and charging cycles. The amorphous carbon coating on the surface of SnO_2 thin film reduced the electrode deterioration, effectively improved the conductivity, electrochemical stability of the electrode in LIBs.

***Keywords*:** SnO_2; magnetron-sputtering; thin film; carbon-coating; Li-ion storage

*Corresponding author at: School of Materials Science and Engineering, Central South University, Changsha 410083, P.R. China; Tel.: +86-731-8887 7740; Fax: +86-731-8887 6692. E-mail address: zhchli@csu.edu.cn (Zhicheng Li)

RSC Advances Accepted Manuscript

1. Introduction

Lithium-ion batteries (LIBs) are the most popular rechargeable batteries in consumer electronics. Portable electronic devices rely largely on the high energy density, high electromotive force and long cycle life of these batteries, whose performance, on the other hand, is unlikely to meet the requirements for future technological improvements on grid storage, electric vehicles and hybrid electric vehicles. [1-3] Despite the fair stability and rate performance of currently commercialized graphite anode, its low specific capacity has hindered its further development, thus having stimulated extensive researches for anode substitutes.

Much work has been devoted to alloying-type tin-based anodes, SnO_2 in particular. Two principle electrochemical processes occur in SnO_2 based anodes during charge-discharge cycling: [4]

$$SnO_2 + 4Li^+ + 4e^- \leftrightarrow Sn + 2Li_2O \quad (1)$$

$$Sn + xLi^+ + xe^- \leftrightarrow Li_xSn \ (0 \leq x \leq 4.4) \quad (2)$$

The complete discharging processes comprise the reduction of SnO_2 and alloying of metallic Sn to $Li_{4.4}Sn$, which lead to a whole discharge capacity as high as 1491 $mAh \cdot g^{-1}$ (782 $mAh \cdot g^{-1}$ theoretically reversible as shown in Eq. (2)). [5] The high theoretical capacity is quite intriguing yet alloying-dealloying processes always accompany intractable volume change up to 250%. [6,7] Inevitably, mechanical structure of the anode materials fails and active materials lose contact with the current collector, causing severe capacity fading.

Hybridizing SnO_2 with buffering materials such as carbon, Cu and conducting polymers is an effective method to tackle the aforementioned problems whilst

RSC Advances Accepted Manuscript

improving conductivity of SnO_2. [8-12] Carbon has won a reputation in either anode or cathode surface coating owing to its high stability and compatibility, which stimulated extensive study and utilization in composite electrodes by various techniques. Typical carbon-coating techniques include spray pyrolysis, wet chemical method, hydrothermal/solvothermal methods, calcination after polymer coating, sol-gel reaction, *etc.* [13-17] These approaches generally involve a mixture of carbon precursor and base material in the preparation process, during which the precursor might induce unwanted phases or morphologies. [18] Some methods, for instance, hydrothermal method, usually require additional treatment that adds liability to the product. [19] It has been reported that nano-scaled Sb-doped SnO_2 deposited by magnetron sputtering on copper foil has excellent electrochemical performance as anode material. [20] With magnetron sputtering technique, thin films of different composition and thickness can be easily obtained under well-controlled conditions.

In an attempt to incorporate SnO_2 thin film with carbon coating, SnO_2 is deposited on copper foil by radio frequency (RF) magnetron sputtering and carbon is coated on the surface of the thin film by the same technique in present work. This method provides a new angle on thin film carbon coating to obtain composite materials. The electrochemical properties of the carbon-coated SnO_2 thin film are investigated and its microstructure is inspected by transmission electron microscopy (TEM).

2. Experimental

The preparation of SnO_2 target for sputtering was conducted by a traditional ceramic fabrication process. [20] After sol-gel synthesis, calcination, cold pressing, sintering and polishing, a target was obtained, 50 mm in diameter and 4 mm in

RSC Advances Accepted Manuscript

thickness. Copper foil substrates were initially ultrasonically cleaned in ethanol and then deposited with SnO_2 thin films by RF magnetron sputtering (JGP 450, China) at room temperature. The sputtering chamber was evacuated to a base pressure of 5.0×10^{-4} Pa and then maintained at 0.8 Pa by adjusting Ar/O gas mixture at a flux ratio of 4:1 during sputtering, which includes 30 minutes of pre-sputtering to ensure a clean target surface and stable glow and 60 minutes of film production. Next, carbon was coated on top of SnO_2 film with graphite target by the same technique; differently though, the sputtering atmosphere was pure argon and the sputtering time was 3 minutes. The carbon-coated SnO_2 (CCSO) thin films were cut into round pieces of 12 mm in diameter and assembled in half coin cells (CR 2032), in an argon-filled glove box, with Li metal foil as counter electrode and reference electrode. The electrolyte is 1 M $LiPF_6$ solution in a mixture of ethylene carbonate (EC) and diethyl carbonate (DEC) with a volume ratio of 1:1.

Galvanostatic charge-discharge processes were performed on a battery measurement system (Land CT2001A, China) at room temperature. The cells were cycled between 0.01 V and 2.00 V *vs.* Li/Li^+ at a current density of 0.1 C. For rate performance, the cells were tested on the same system at current densities of 0.1 C, 0.2 C, 0.4 C, 0.8 C, 1 C in sequence and 0.1 C again, for 10 cycles at each current density. Cyclic voltammetry (CV) was carried out on an electrochemistry workstation (Gamry Reference 600, USA) at a scanning rate of 0.1 mV s^{-1} between 0.01 V and 2.00 V. The instrument was also used to measure the electrochemical impedance in order to determine the conduction characteristics of the assembled cells.

Scanning electron microscope (SEM, FEI Quanta 650 FEG) was employed to study

RSC Advances Accepted Manuscript

the configuration and thickness of CCSO composite thin film from both plain and cross-sectional views. The sample for cross-sectional view was obtained by ripping the thin film along a cutting crack. The surface morphology of a clean copper foil was also observed under SEM for comparison. The microstructures and phase components of the SnO_2 thin films and CCSO thin films were inspected by a transmission electron microscope (TEM, FEI Tecnai G^2 F20) before and after being electrochemically induced. Cells discharged to 0.01 V or charged to 2.00 V were dismantled respectively, and the active materials were elaborately prepared on holey carbon grids for TEM investigation, as was the pristine CCSO material. [21,22] Fast Fourier Transform (FFT) analysis was also performed on the high-resolution images to determine the reaction products after the cycling.

3. Results and discussion

3.1 Microstructure of carbon-coated SnO_2 thin film

Fig. 1(a) shows the SEM image of a pristine CCSO thin film, where the right part is the surface morphology of the CCSO film, the upper-left inset is the cross-sectional view of CCSO thin film, and the lower-left inset is a plain-view surface morphology of a clean copper foil. The CCSO thin film exhibits in the form of cauliflower-shaped protrusions which are uniformly distributed on the surface of copper foil. Compared with the clean copper foil (lower-left inset), it can be decided that these protrusions stemmed from the crude surface of the copper foil when SnO_2 was sputtered onto it. The thickness of active material layer is uniformly less than 1 μm as can be seen in upper-left inset, while the size of protrusions varies under 5 μm with substantial ravines between them, which can increase the contact area of active material and electrolyte. Carbon layer cannot be indentified in either plain or cross-

RSC Advances Accepted Manuscript

sectional images for its limited thickness. The SEM results provide the evidence that the as-prepared CCSO thin film is uniform on the substrate and that the structural characteristic with cauliflower-shaped protrusions and ravines should be advantageous for the application in lithium-ion batteries. [23]

Fig. 1(b) presents the TEM investigations of a pristine CCSO thin film. The upper-right inset is the selected area electron diffraction (SEAD) pattern and the lower-left inset is the high-resolution TEM (HRTEM) image featuring carbon layer. The diffraction rings in the SEAD are indexed as polycrystalline SnO_2 ($P4_2/mnm$, $a = b = 4.74$ Å, $c = 3.18$ Å) with a nanostructured characteristic. The average size of SnO_2 crystals is estimated to be about 5 nm from HRTEM image. An evenly distributed thin layer of amorphous carbon can be seen in Fig. 1(b). The thickness of coated carbon layer is about 3-5 nm, insignificant to affect the structure of mass SnO_2 material. Through FFT analysis of HRTEM image, the lattice fringe of 3.350 Å is indexed to {110} plane family of tetragonal SnO_2, confirming the pristine structure of tin dioxide.

3.2 Electrochemical performance

Fig. 2 illustrates the first three cycles of CV of the CCSO (Fig 2(a)) and pure SnO_2 (Fig 2(b)) thin films. The CV characteristic of CCSO thin film is generally in accordance with that of the SnO_2 one without carbon coating, indicating that the means magnetron-sputtered carbon coating has negligible effect on the reaction mechanisms of SnO_2 anode material. To be specific, three peaks emerge during the first discharging process at around 0.94 V, 0.52 V and 0.20 V, respectively, and two during the first charging process at around 0.52 V and 1.32 V, marked in sequence as P1-P5 as shown in Fig. 2(a). Broad and sharp P1 is ascribed to the reduction of SnO_2 to Sn and consequent formation of LiO_2, corresponding to the reaction in Eq. (1). This

RSC Advances Accepted Manuscript

partially reversible reaction results in a large initial capacity loss, which manifests as the obviously weak peaks around P1 in later cycles. Its counter peak P5 is duly weak and broad in three cycles. P2 and P3 should be signs of a two-step lithium insertion for the alloying as shown in Eq. (2) and may also involve the formation of solid-electrolyte interface (SEI) layer. Research by Zhang *et al.* has evidenced that carbon coating can stabilize SEI layer and restrain its thickness during repetitive lithiation and delithiation, leading to a better environment for active materials. [24] Therefore, it can be inferred that no significant capacity loss is attributed to SEI layer in the later cycles. As for de-alloying of $Li_{4.4}Sn$, which is a one-step lithium extraction process, a broad P4 in charging process correlates with P3 and P2 with equivalent current intensity. [25] On the whole, except for P1, all the peaks show a considerable augmentation in current intensity in second and third cycles, indicating an activation process in anode material, probably induced by carbon coating. Although the thin layer of carbon can fortify anode nanostructure and does not affect the electrochemical reactions of SnO_2, it somehow impedes full utilization of anode material at first few cycles. This is also revealed in cycling performance and will be discussed later in this section.

Fig. 3 compares the electrochemical impedance spectra (EIS) of the CCSO and pure SnO_2 thin films in the assembled cells, in the frequency range of 1 Hz – 1 MHz. Both spectra are comprised of a compressed arc at high frequencies and a tail at low frequencies. The tail is attributed to Warburg diffusion. The ohmic resistances (indicated by the high frequency intercept of real axis) are close to each other and are very small, but the arcs are of different diameters, suggesting different values of charge transfer resistances (R_{ct}). [26] R_{ct} of CCSO cell is about half of that of the pure

RSC Advances Accepted Manuscript

SnO_2 one. The EIS results demonstrate that carbon coating efficiently improves the conductivity of the cell for the charge transport.

The cycling performance and Coulombic efficiency of CCSO thin film are illustrated in Fig. 4(a) and compared with those of pure SnO_2 thin film as shown in Fig. 4(b). Both anode materials show a low specific capacity during first few cycles, indicating an activating process in the electrodes. The activation process should be attributed to the deficiency of electrolyte permeation into the composite thin film. As shown in Fig. 1, the CCSO thin film has numerous ravines between the cauliflower-shaped protrusions (see in Fig. 1(a)), and the SnO_2 active materials are coated by amorphous carbon layer (see in Fig. 1(b)). Therefore, the electrolyte might not easily permeate into the whole active materials in the electrode in the first few cycles. The possible solution to this phenomenon might to prolong the age time before the assembled cells are applied to charging-discharging, or to use more electrolyte liquid in the cells when assembling. Given enough time and/or electrolyte, the ravines are more likely to be filled with electrolyte, leading to faster activation of the reaction between electrolyte and the active material. [27]

The specific charge capacity of CCSO electrode reaches the maximum value of 858 $mAh \cdot g^{-1}$ at the 7^{th} cycle, while that of pure SnO_2 reaches 1049 $mAh \cdot g^{-1}$ at 3^{rd} cycle. The specific discharge capacity follows the same pattern for both materials, with highest values of 906 $mAh \cdot g^{-1}$ at 5^{th} cycle and 1099 $mAh \cdot g^{-1}$ at 3^{rd} cycle for CCSO and pure SnO_2, respectively. Nevertheless, specific capacity of pure SnO_2 fades much faster than the CCSO electrode. Apparently, CCSO thin film was activated more slowly than pure SnO_2 thin film, probably due to a 'barrier effect' caused by carbon

RSC Advances Accepted Manuscript

coating. The carbon layer can obstruct electrolyte from permeating through mass SnO_2, thus impeding complete lithiation and limiting the full utilization of anode material. However, after 100 electrochemical cycles at 0.1 C, only 207 $mAh \cdot g^{-1}$ of specific discharge capacity retains for pure SnO_2, but 650 $mAh \cdot g^{-1}$ for CCSO, corresponding to 19% and 72% of retaining capacity, respectively. Coulombic efficiencies (CE) of both thin films stand low at first few cycles, but increase to *ca*. 99% in subsequent cycles. While CE of the pure SnO_2 thin film starts to decrease after some 70 cycles, however, the CCSO one maintains a high CE of approximately 99% through all 100 cycles, demonstrating superior stability of the anode. In summary, despite the barrier effect of carbon coating on realizing full potential of SnO_2 capacity at the initial cycles, the barrier on the surface of SnO_2 thin film can prevent aggregation of nano-particles and reduce the pulverization caused by volume expansion/shrink during the electrochemical cycling. Furthermore, the highly conductive carbon layer provides good electrical contact and allows for high capacity from active SnO_2 particles at later cycles. [24,28] Magnetron-sputtered carbon layer plays a significant role as structure constraint and prevents SnO_2 from deteriorating and pulverizing owing to its conductive and elastic properties.

Fig. 5 gives some detailed data from charging and discharging analysis of carbon-coated SnO_2 thin film. Fig. 5(a) is the capacity-potential relation at the 5^{th}, 10^{th}, 50^{th} and 100^{th} cycles, respectively, and Fig. 5(b) is the differentiated curves for the related cycles. It is evident from Fig. 5(a) that the electrochemical transition at the 100^{th} cycle follows the similar profile as the 50^{th} cycle, but has altered from the 5^{th} and 10^{th} cycles, with various slopes and plateaus at different potentials. These differences are amplified when demonstrated as differentiated capacity curves in Fig. 5(b). At the 5^{th}

RSC Advances Accepted Manuscript

and 10th cycles, three peaks marked by S1, S2 and S3 show up during discharging at potentials of 0.94 V, 0.56 V and 0.24 V, respectively, while only two peaks marked by S4 and S5 show up during charge at 0.47 V and 1.35 V, respectively. These two cycles are in good agreement with the 2nd and 3rd cycles of CV results, with the discharge peaks slightly shifting to higher potentials. Representing a pair of partially irreversible reactions, both S1 and S5 peaks decline at the 50th cycle as expected, and S2 and S3 keep shifting and turn up at 0.60 V and 0.45 V, respectively. The interesting phenomenon is that S4 splits into two peaks (marked as S4′ and S4″ in Fig. 5(b) at 0.47 V and 0.62 V, respectively), matching with discharge peaks S3 and S2. [25] Apparently, the lithiation and delithiation in this electrode system are two-step redox reactions which are highly reversible even after 100 cycles. The intermediate products can be various lithium-tin compounds such as Li_7Sn_3, Li_5Sn_2 and Li_7Sn_2 as reported by Ouyang et al. in Sb-doped SnO_2 thin films. [20,29] The charge-discharge manner is quite clear and stable at the 50th cycle and maintains well into the 100th cycles, with only a minor loss of specific discharge capacity of 25 mAh·g^{-1}. The superior stability of the anode material might reflect the advantage of carbon-coating on the SnO_2 thin film.

To examine the stabilizing function of the carbon coating on the LIBs, cells with CCSO anode were tested at different current densities and the results are shown in Fig. 6. The activation process can still be seen at first few cycles. The specific discharge capacity declines from the highest of 1065 mAh·g^{-1} at the 4th cycle at 0.1 C to 625 mAh·g^{-1} at the 50th cycle at 1 C, and bounces back to 763 mAh·g^{-1} at 60th cycle when current density was switched to 0.1 C again for 10 cycles. The CCSO thin film preserves a high capacity even at relatively high rates. The results once again prove

RSC Advances Accepted Manuscript

that magnetron-sputtered carbon coating is an effective way to improve stability of SnO_2 thin film as anode in LIBs.

3.3 Carbon coating through phase transition

It is important for carbon layer to be durable and to sustain the anode structure through repetitive discharge and charge. Therefore, TEM was further employed to examine the carbon durability and elucidate lithiation and delithiation in the CCSO anode material. Figs. 7(a) and 7(b) show HRTEM images of the CCSO thin films discharged to 0.01 V and charged to 2.00 V after 10 cycles, respectively. The HRTEM images were performed FFT as given in the related insets, where the dashed rings mark out diffraction rings of relevant phases. Carbon layer is still found intact on the surface of SnO_2 after 10 cycle electrochemical processes. The thickness of carbon layer largely stays the same as before cycling (3-5 nm), indicating unreactivity and excellent mechanical property. On the other hand, the grains become rather small and indistinct because the electrochemical cycles lead to crystallite fragmentation.

Through analysis of FFT image in Fig. 7(a), the grains are determined to be $Li_{4.4}Sn$. After the anode is discharged to 0.01 V, SnO_2 is completely reduced to metallic Sn and metallic Sn is fully alloyed with Li^+ to form $Li_{4.4}Sn$, as shown in Eqs. (1) and (2). Lattice spacings of two grains are identified as {264} (shown in the inset enlarged picture) and {440} plane families of $Li_{4.4}Sn$ phase. In Fig. 7(b), when the anode is charged to 2.00 V, the diffraction rings in the inset are indexed to {110}, {101}, {201} and {211} plane families of SnO_2 while some spots are indexed to {101} plane family of Sn. Two representative grains are marked out as SnO_2 {110} plane family of 3.350 Å in plane spacing and Sn {101} plane family of 2.792 Å. Lithium ions extract from

RSC Advances Accepted Manuscript

$Li_{4.4}Sn$ and the alloy is reverted to Sn and SnO_2 during charging process. Since the 10^{th} cycle is still an early stage of cycling, it is reasonable for Sn to be partially oxidized to SnO_2 in this process. HRTEM images provide solid evidence that The CCSO thin film complies with Eqs. (1) and (2) during cycling under firm and continuous structural protection provided by magnetron-sputtered carbon layer on the surface.

4. Conclusion

A layer of amorphous carbon with the thickness of 3-5 nm was sputtered on the surface of SnO_2 thin film by RF magnetron sputtering. The carbon-coated SnO_2 thin film for the anode material of lithium-ion batteries exhibits high specific discharge capacity and retention rate, and has the electrochemical performance much higher than that of the pure SnO_2 thin film. The carbon coating maintains the original structure during the electrochemical processes. Carbon layer imposes a barrier effect on electrolyte permeation and may hamper full utilization of active SnO_2 material, but it effectively fortifies SnO_2 nano-structure and ensures good rate performance. The present work offers a new method for preparing directly carbon-coated thin film without incurring unwanted phases or morphologies, and the carbon coating is an effective method to improve electrochemical properties of an electrode in LIBs.

Acknowledgments

The authors acknowledge the support of the National Nature Science Foundation of China (No. 51172287) and the Laboratory Research Fund by the State Key Laboratory of Powder Metallurgy, Central South University, China.

RSC Advances Accepted Manuscript

References

[1] B. Dunn, H. Kamath, J. M. Tarascon, *Science*, 2011, **334**, 928-935.

[2] M. M. Thackeray, C. Wolverton, E. D. Isaacs, *Energ. Environ. Sci.*, 2012, **5**, 7854-7863.

[3] X. W. Lou, D. Deng, J. Y. Lee, L. A. Archer, *Chem. Mater.*, 2008, **20**, 6562-6566.

[4] I. A. Courtney, J. R. Dahn, *J. Electrochem. Soc.*, 1997, **144**, 2045-2052.

[5] Y. Idota, T. Kubota, A. Matsufuji, Y. Maekawa, T. Miyasaka, *Science*, 1997, **276**, 1395-1397.

[6] J. Y. Huang, L. Zhong, C. M. Wang, J. P. Sullivan, W. Xu, *Science*, 2010, **330**, 1515-1520.

[7] J. M. Whiteley, J. W. Kim, C. S. Kang, J. S. Cho, K. H. Oh, S. H. Lee, *J. Electrochem. Soc.*, 2015, **162**, A711-A715.

[8] M. Ara, K. Wadumesthrige, T. Meng, S. O. Salley, K. S. Ng, 2014, *RSC Adv.*, 2014, **4**, 20540-20547.

[9] J. S. Chen, Y. L. Cheah, Y. T. Chen, N. Jayaprakash, S. Madhavi, Y. H. Yang, X. W. Lou, *J. Phys. Chem. C*, 2009, **113**, 20504-20508.

[10] H. El-Shinawi, M. Böhm, T. Leichtweiß, K. Peppler, J. Janek, *Electrochem. Commun.*, 2013, **36**, 33-37.

[11] L. Yuan, J. Wang, S. Y. Chew, J. Chen, Z. P. Guo, L. Zhao, K. Konstantinov, H. K. Liu, *J. Power Sources*, 2007, **174**, 1183-1187.

[12] Y. Zhao, X. Li, B. Yan, D. Li, S. Lawes, X. Sun, *J. Power Sources*, 2015, **274**, 869-884.

[13] L. Yuan, K. Konstantinov, G. X. Wang, H. K. Liu, S. X. Dou, *J. Power Sources*, 2005, **146**, 180-184.

[14] T. Moon, C. Kim, S. T. Hwang, B. Park, *Electrochem. Solid. St.*, 2006, **9**, A408-A411.

[15] X. Sun, J. Liu, Y. Li, *Chem. Mater.*, 2006, **18**, 3486-3494.

[16] M. S. Park, Y. M. Kang, J. H. Kim, G. X. Wang, S. X. Dou, H. K. Liu, *Carbon*, 2008, **46**, 35-40.

[17] B. Zhou, S. Yang, L. Wu, W. Wu, W. Wei, L. Chen, H. Zhang, J. Pan, X. Xiong, *RSC Adv.*, 2015, **5**, 49926-49932.

[18] J. Wang, J. Yang, Y. Tang, J. Liu, Y. Zhang, G. Liang, M. Gauthier, Y. K. Chen-Wiegart, M. N. Banis, X. Li, R. Li, J. Wang, T. K. Sham, X. Sun, *Nat. Commun.*, 2014, **5**, 3415.

[19] G. Wu, Z. Li, W. Wu, M. Wu, *J. Alloy. Compd.*, 2014, **615**, 582-587.

[20] P. Ouyang, H. Zhang, Y. Wang, W. Chen, Z. Li, *Electrochim. Acta*, 2014, **130**, 232-238.

[21] W. Chen, H. Zhang, Z. Ma, B. Yang, Z. Li, *J. Mater. Chem. A.*, 2015, **3**, 14202-14209.

[22] Z. Ma, H. Zhang, Y. Zhang, J. Zhang, Z. Li, *Electrochimi. Acta*, 2015, **176**, 1427-1433.

RSC Advances Accepted Manuscript

[23] C. Zhang, X. Peng, Z. Guo, C. Cai, Z. Chen, D. Wexler, S. Li, H. Liu, *Carbon*, 2012, **50**, 1897-1903.

[24] W. M. Zhang, X. L. Wu, J. S. Hu, Y. G. Guo, L. J. Wan, *Adv. Funct. Mater.*, 2008, **18**, 3941-3946.

[25] W. Xu, N. L. Canfield, D. Wang, J. Xiao, Z. Nie, *J. Power Sources*, 2010, **195**, 7403-7408.

[26] L. Wang, D. Wang, Z. Dong, Z. Dong, F. Zhang, J. Jin, *Nano Letters*, 2013, **13**, 1711-1716.

[27] S. H. Lee, S. H. Yu, J. E. Lee, A. Jin, Lee, D. J. Lee, N. Lee, H. Jo, K. Shin, T. Hyeon, *Nano Letters*,**13**, 4249-4256.

[28] H. Li, H. Zhou, *Chem. Commun.*, 2012, **48**, 1201-1217.

[29] P. Ouyang, H. Zhang, W. Chen, Y. Wang, Y. Zhang, Z. Li, *Mater. Res. Bull.*, 2015, **61**, 9-15.

RSC Advances Accepted Manuscript

Figure Captions

Fig. 1 Microstructure investigations of the pristine carbon-coated SnO_2 (CCSO) thin film sputtered on copper foil, (a) SEM observations, where the right part is the surface morphology of the CCSO film, the upper-left inset is a cross-sectional view of CCSO thin film, and the lower-left inset is a plain-view surface morphology of a clean copper foil. (b) TEM observations, the upper-right inset is a related SEAD pattern and the lower-left inset is an HRTEM image.

Fig. 2 First three cycles of CV curves of the assembled cells with thin film as test electrode, (a) carbon-coated SnO_2 thin film, (b) pure SnO_2 thin film.

Fig. 3 Electrochemical impedance spectra of the cells with CCSO thin film and pure SnO_2 thin film as tested electrodes, respectively, measured in the frequency range of 1 Hz – 1MHz.

Fig. 4 Cycling performances of thin films at 0.1C for 100 cycles, (a) carbon-coated SnO_2 thin film, (b) pure SnO_2 thin film.

Fig. 5 Electrochemical features of carbon-coated SnO_2 thin film at 5^{th}, 6^{th}, 50^{th} and 100^{th} cycles, (a) plots of capacity *vs.* potential, (b) differentiated capacity *vs.* potential relations.

Fig. 6 Rate performance of carbon-coated SnO_2 thin film at current densities of 0.1C, 0.2C, 0.4C, 0.8C and 1C.

Fig. 7 HRTEM investigations of carbon-coated SnO_2 thin films after 10 electrochemical cycles, carbon layer is still found intact on the surface of anode material. The insets are FFT images of each HRTEM image. (a) discharged to 0.01 V, (b) charged to 2.00 V.

RSC Advances Accepted Manuscript

Figure 1

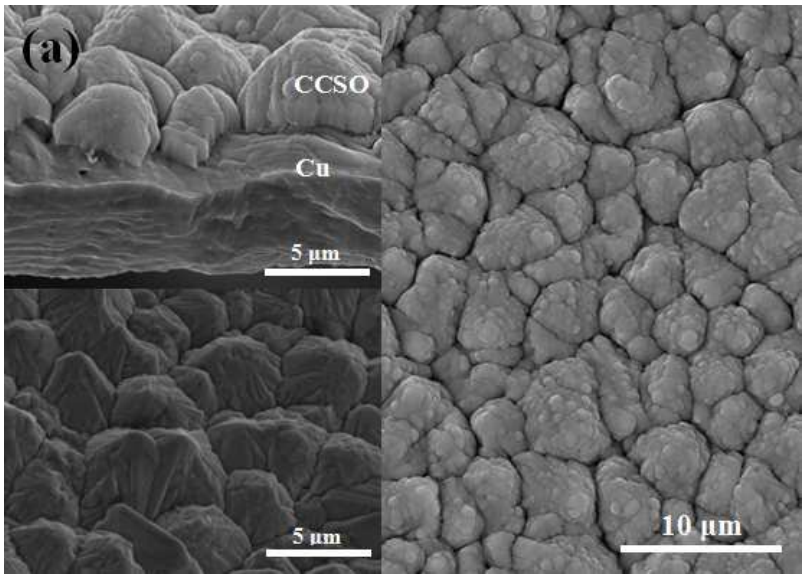

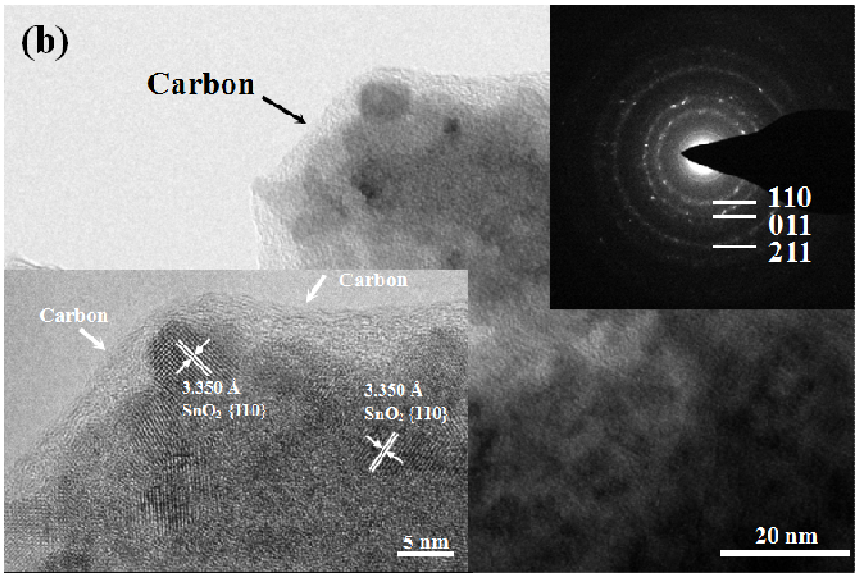

RSC Advances Accepted Manuscript

Figure 2

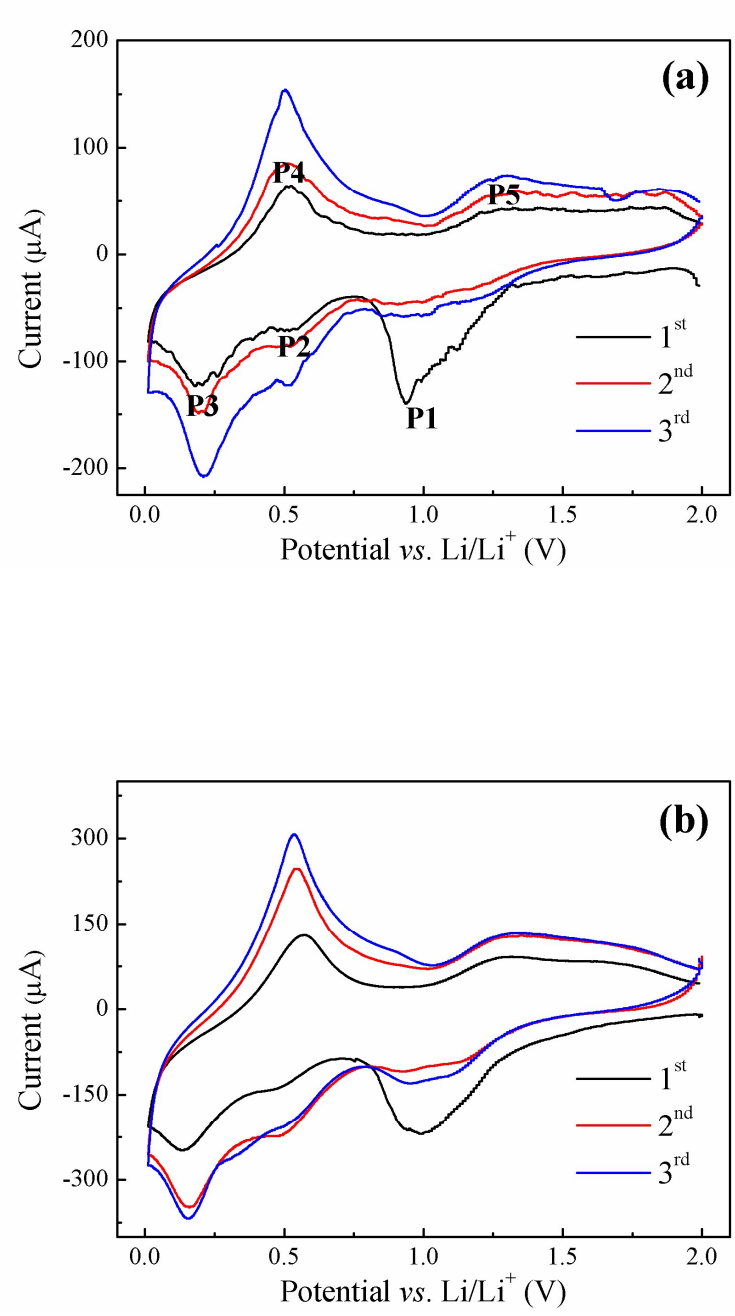

RSC Advances Accepted Manuscript

Figure 3

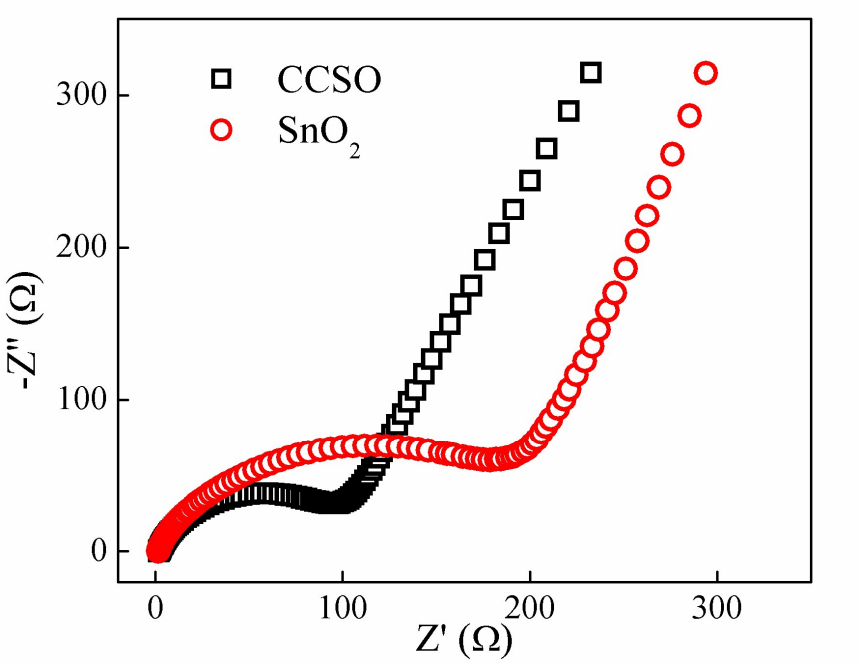

RSC Advances Accepted Manuscript

Figure 4

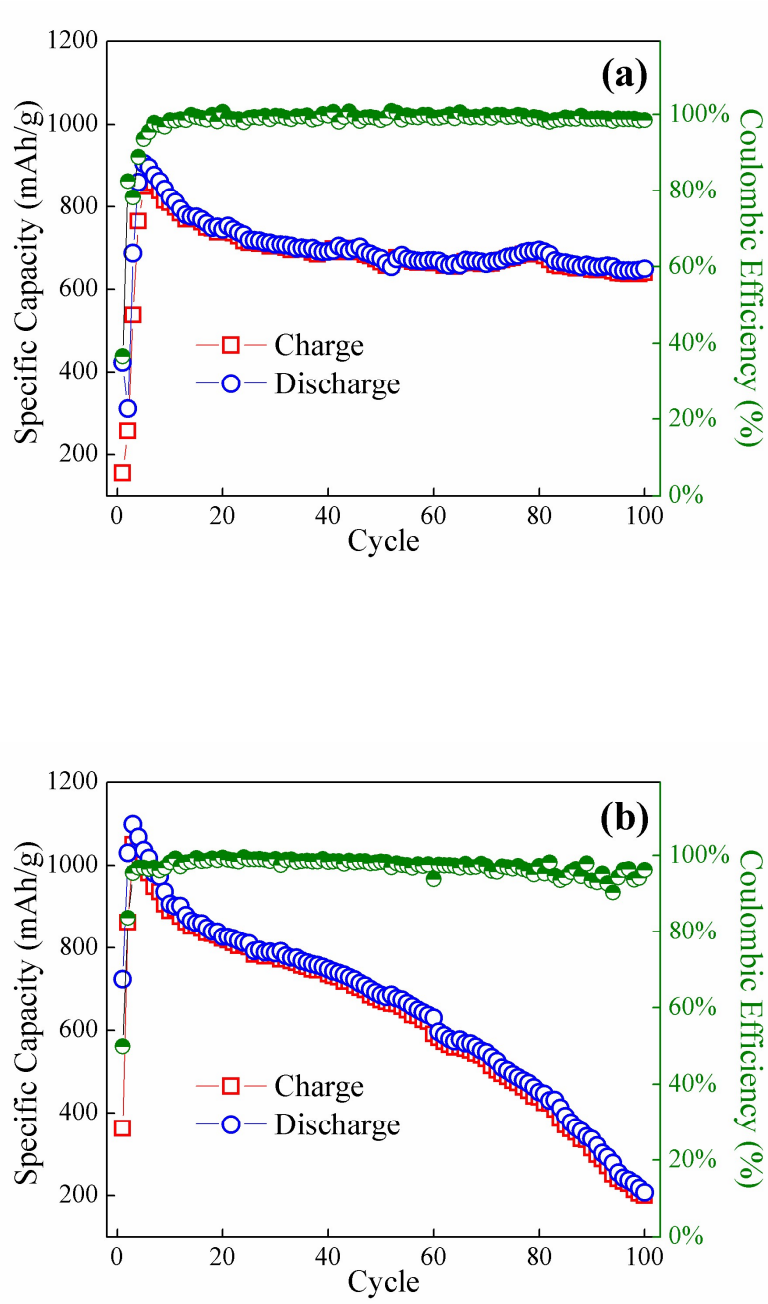

RSC Advances Accepted Manuscript

Figure 5

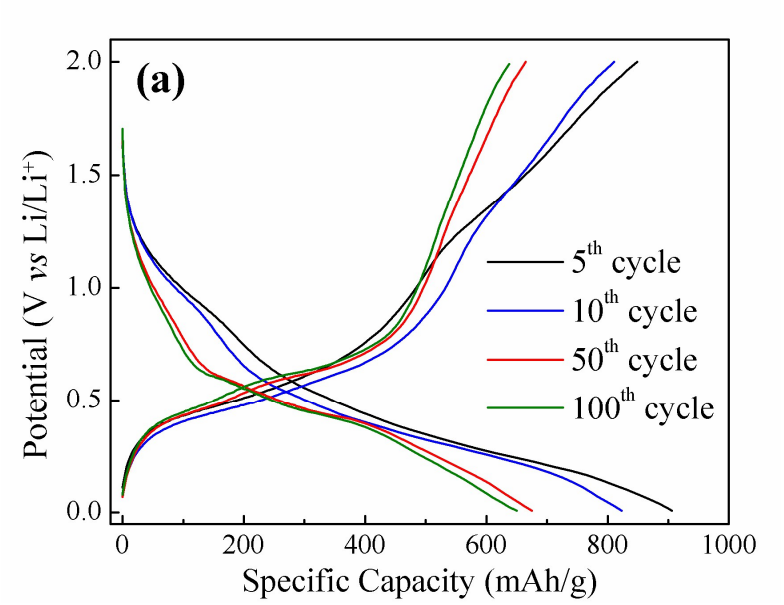

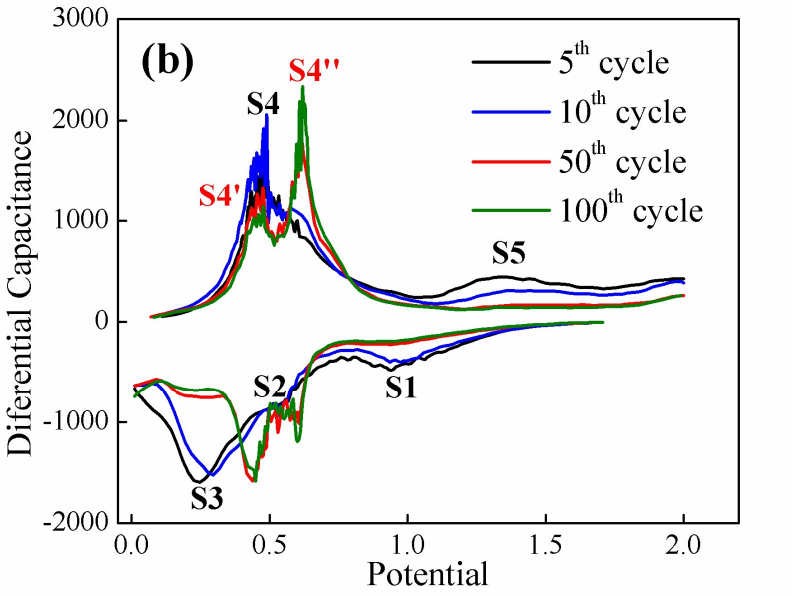

RSC Advances Accepted Manuscript

Figure 6

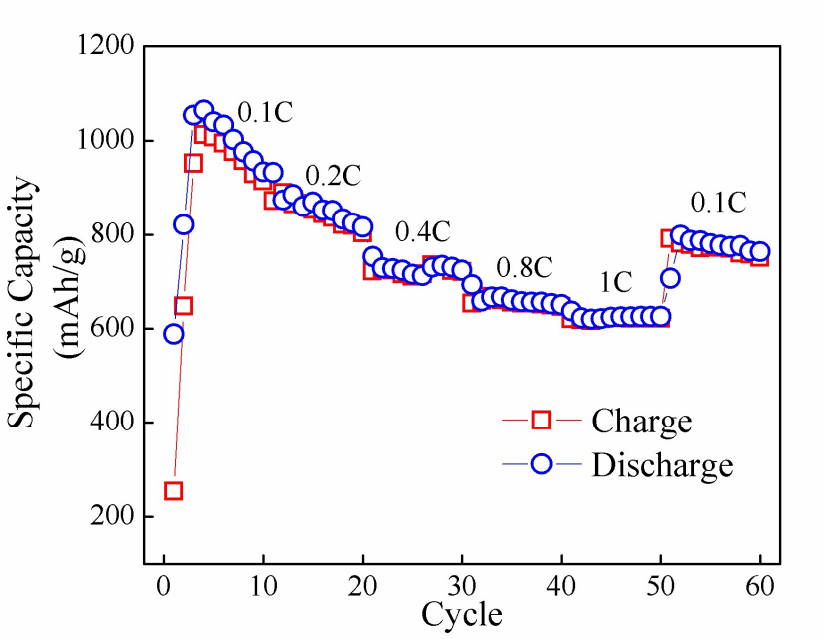

RSC Advances Accepted Manuscript

Figure 7

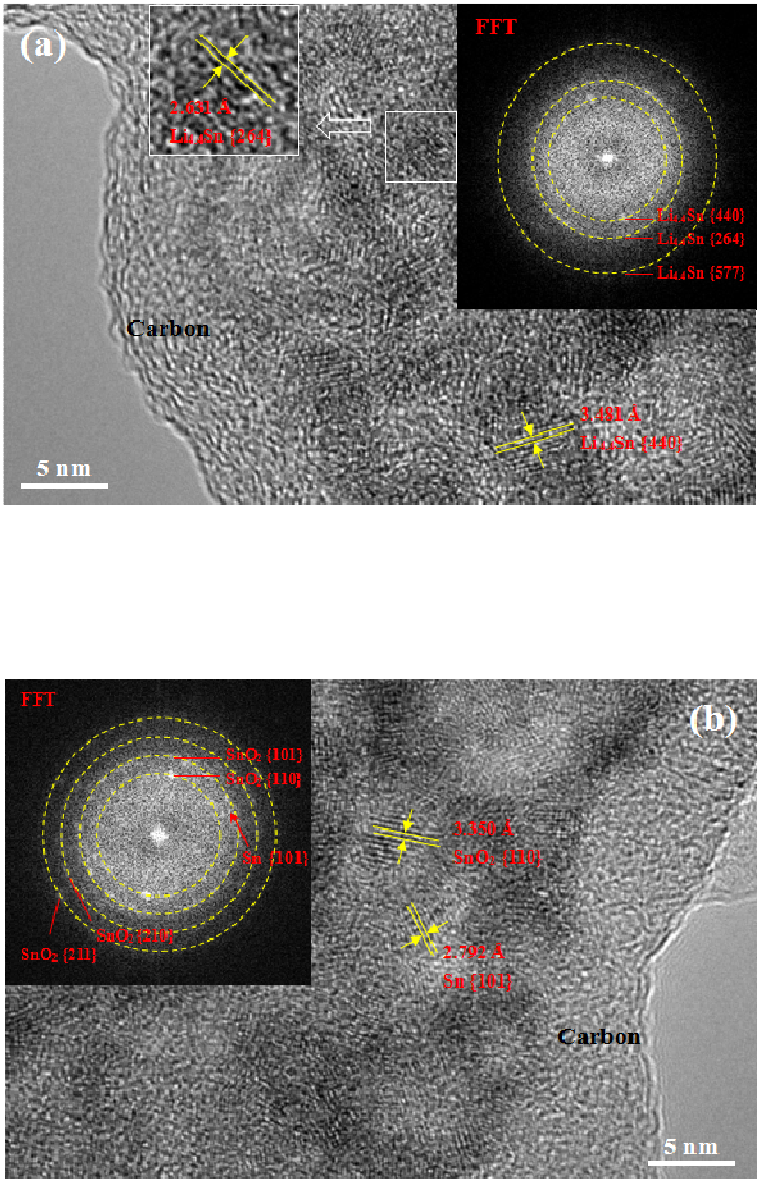

RSC Advances Accepted Manuscript

Highlights

1. SnO_2 thin films coated with amorphous carbon layer with the thickness of 3-5 nm.
2. Carbon coating shows excellent durability and reduces the electrode deterioration.
3. Carbon coating improves the conductivity, electrochemical stability.

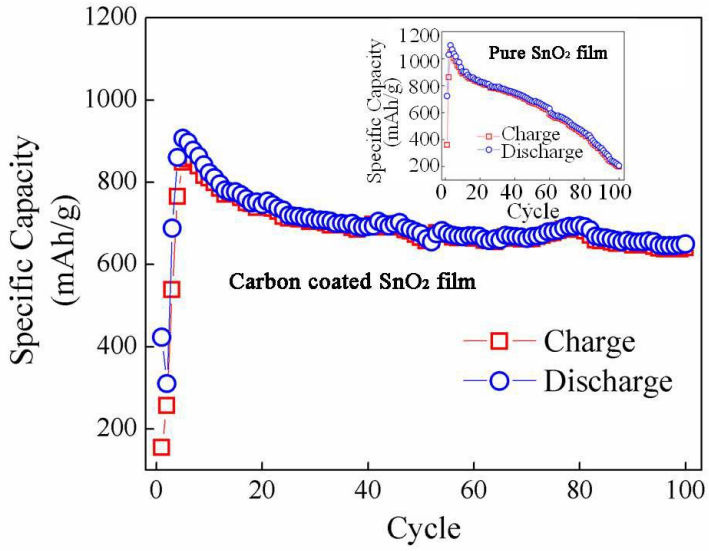

Graphical abstract: Carbon coating on SnO_2 thin film reduced the electrode deterioration, improved the conductivity and electrochemical stability

RSC Advances Accepted Manuscript